Chapter 24
Homonuclear 3D NMR of Biomolecules

Rolf Boelens and Robert Kaptein

NMR Spectroscopy Research Group, Bijvoet Center for Biomolecular Research, Utrecht University, Bloembergengebouw, Padualaan 8, 3584 CH Utrecht, The Netherlands

24.1 Introduction 315
24.2 Why Higher Dimensions? 316
24.3 Classification of Multidimensional NMR Experiments 317
24.4 The Design of Multidimensional Homonuclear Experiments 317
24.5 Selective and Nonselective Homonuclear 3D NMR 318
24.6 Principles of Homonuclear 3D Spectroscopy 319
24.7 Practical Aspects 320
24.8 Applications 323
24.9 Prospects for 3D NMR Spectroscopy 330
References 331

24.1 INTRODUCTION

High-resolution NMR can be used for determining structures of small biomolecules in solution.[1] Such studies are based upon the measurement of interactions between protons. The NOE, the origin of which is dipolar cross-relaxation between protons, is especially crucial since it can be used to determine distances between closely spaced protons. The other proton–proton interaction is the J-coupling, which is used to identify spin systems during the resonance assignment stage but which can also give information on torsion angles, and in this way leads to more accurate structures. For small biomolecules these proton–proton interactions are most conveniently measured by 2D NMR techniques.[2] Thus, the J-coupling manifests itself as cross peaks in COSY and TOCSY (or 2D HOHAHA) spectra and the NOE as cross peaks in NOESY (or 2D NOE) spectra (see Chapters 12, 13, 16 and 18).

Except for some favorable cases, however, 2D NMR studies have been limited to small biomolecules with molecular masses of less than 12 kDa. Several problems arise with larger molecules. Both the number of proton resonances and the resonance linewidth increase with size. This leads to overlap of resonances, which prohibits the unambiguous assignment of 2D cross peaks to specific proton pairs. The spectral resolution can be increased by adding a third[3–8] or even a fourth frequency domain.[9,10] In this way, overlapping protons can be characterized with the additional frequency of an associated nucleus that will help in establishing the interpretation of cross peaks. An extra complication is, however, that due to the increase in linewidth for large biomolecules, it becomes more difficult to observe small proton–proton J-couplings and that magnetization transfer in 3D spectra based on such J-couplings becomes weak. This disadvantage may be overcome in homonuclear 3D NOESY–NOESY spectroscopy,[11] but the complexity of the 3D NOESY–NOESY spectra can be high and their sensitivity low. More recently, a number of heteronuclear 3D experiments

have been developed, such as 3D NOESY–HMQC, 3D TOCSY–HQMC[12–15] and 3D triple resonance techniques for (^{13}C, ^{15}N) doubly labeled molecules (see next Chapter).[16,17]

These heteronuclear techniques overcome the aforementioned problems, because they rely on strong heteronuclear J-coupling constants and because the magnetization transfer is unique in many cases. The sensitivity of heteronuclear 3D and 4D experiments can be high and the spectral complexity low, and there is no doubt that for large biomolecules such methods are preferable to the homonuclear ones. However, the heteronuclear techniques have one clear disadvantage. They require that the biomolecular material is enriched in ^{13}C, ^{15}N or both isotopes, which is problematic if the material can only be obtained in low yields or if the biomolecule cannot be isolated from cell cultures. This applies to a large group of very interesting biomolecules, including glycoproteins, oligosaccharides, and oligonucleotides.

Several reviews on multidimensional NMR techniques have appeared, and a thorough account of various theoretical and practical aspects of 3D NMR has been given by Griesinger *et al*.[18] Triple resonance techniques for studies on (^{13}C, ^{15}N) doubly labeled proteins have been reviewed thoroughly by Clore and Gronenborn[19] and by Bax and Grzesiek.[20] A recent survey was provided by Oschkinat *et al*.[21] Our main focus will be homonuclear 3D NMR of biomolecules; heteronuclei are dealt with in the next two Chapters.

24.2 WHY HIGHER DIMENSIONS?

Most interactions in NMR spectroscopy are pairwise by nature. In principle, two frequency domains and, thus, 2D NMR should suffice to establish such pair interactions between magnetic nuclei.[22] Certainly for large biomolecules, however, there is a high chance of overlap for resonances of different nuclei. In that case 2D relayed experiments have been proposed, where the magnetization is transferred from the second overlapping nucleus to a third one via an additional mixing step.[23,24] Both homonuclear and heteronuclear coherence transfer steps can be used to resolve ambiguous NOEs in a new frequency domain.[25–28] For small biomolecules the comparison of resonances in the direct domain of the original 2D experiment and the indirect domain of the 2D relay experiment is in many cases sufficient to resolve most ambiguities.[29] However, for large molecules it is likely that a new overlap exists in this indirect domain. This overlap may then be resolved by a simultaneous registration of the direct and the relayed frequencies. In this way a 3D spectrum is created where overlap for the receiving nuclei can be resolved (Figure 24.1). If overlap exists for the originating nuclei, the magnetization in their domain may also be relayed. Modulation at both the direct and the relayed frequencies for the originating and the receiving nuclei would lead to a 4D spectrum. Higher dimensionality is probably not practical.[20,22]

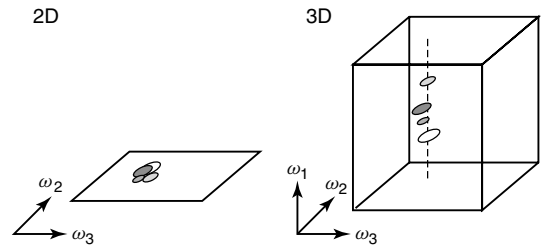

Figure 24.1. Illustration of the increase in resolution due to the increase in dimensionality. In the 2D spectrum four cross peaks overlap. By correlation with a third resonance frequency each cross peak achieves a different position along a line in the 3D spectrum, thus resolving the overlap problem.

In multidimensional NMR one can distinguish between the interactions of interest and those that are suitable for relaying the information to other frequency domains. The structure determination of biomolecules is mainly based on the interpretation of proton–proton NOEs, while for the prerequisite assignment of proton resonances considerable use is made of J-coupling data. Therefore, it is of great importance to establish the absence and presence of these interactions unambiguously. Optimally, the frequencies connected by the relayed transfer are not linearly correlated, the relayed nuclei involved are abundant, the transfer will be very efficient introducing only low signal losses, all proton resonances can be relayed, and the relay interaction can be interpreted uniquely. In practice this is not the case, but the requirements are best met by combinations of various heteronuclear 3D and 4D experiments on (^{13}C, ^{15}N) doubly labeled compounds. When isotope labeling is not possible, however, homonuclear 3D methods may be preferable, but the analysis of the resulting spectra can be complex. A large part of this review will summarize methods for analyzing such homonuclear spectra.

24.3 CLASSIFICATION OF MULTIDIMENSIONAL NMR EXPERIMENTS

Over the years many pulse sequences have been proposed to establish homonuclear and heteronuclear interactions between pairs of nuclei.[2] Of course, all these pair transfers can be used as building blocks of multidimensional NMR experiments. The interactions in high-resolution ^{1}H NMR can have a coherent or an incoherent nature. Incoherent sources for interaction are kinetic exchange and dipolar cross relaxation, while the homonuclear and heteronuclear J-couplings have a coherent nature. Two types of 2D experiments can be discriminated by which these processes can be measured: the large COSY family for identifying J interactions within spin systems[2,30] and the 2D exchange or NOE category for the analysis of kinetic equilibria,[31] NOESY,[32,33] and ROESY[34,35] effects. Most 2D experiments involve magnetization transfer due to a single type of interaction and thus will fall in one of these two categories. Most 3D experiments (but also relayed 2D experiments) should then belong to combinations of these two. The basic categories for double transfer will be J–J, J–NOE, NOE–J, and NOE–NOE. Of these, the J–NOE and NOE–J type experiments will contain the same information and can be brought into one category. It is obvious that one can classify 3D COSY–COSY,[5,6] 3D COSY–NOESY,[6] 3D NOESY–TOCSY experiments,[7,8] or 3D NOESY–ROESY in one of these groups. Of course, with 4D spectroscopy, or better triple transfer techniques, eight (but only six unique) classes can then already be defined, and for quadruple transfer experiments even 16. In general it can be anticipated that the J–J and J–J–J type experiments should be useful for assignment purposes, while triple transfer J–NOE–J type experiments can be helpful for identifying NOEs.

It is clear that by combination of the "building blocks" used in 2D spectroscopy a countless number of different types of experiments can be constructed.

24.4 THE DESIGN OF MULTIDIMENSIONAL HOMONUCLEAR EXPERIMENTS

Each multidimensional experiment will start with a preparation period. Generally, this is a delay to bring the spin system to Boltzmann equilibrium followed by a 90° rf pulse. This will be followed by one or more evolution periods and a detection period, all separated by magnetization transfer steps similar to those in two-dimensional NMR. The experiments can be designed by the appropiate combination of two 2D NMR pulse schemes. A 3D NMR experiment can be regarded as the combination of two 2D experiments, in which the detection period of the first experiment has been replaced by the evolution, mixing, and detection periods of the second.[5] For example, a NOESY and TOCSY experiment can combine to form a 3D NOESY–TOCSY experiment.[7,8] As shown in Figure 24.2, the FID in the time domain t_3 is then recorded as a function of two variable times t_1 and t_2, which are independently incremented. After Fourier transformation in the three dimensions a 3D NMR spectrum is obtained with three independent frequency axes. A cross peak in the 3D spectrum arises when magnetization of one proton is transferred during the first (NOE) mixing period to a second proton and then during the second (TOCSY or HOHAHA) mixing period to a third one. Figure 24.3 shows a number of 3D pulse schemes and their division into preparation, evolution, and mixing periods, but basically the same principles apply to all experiments.

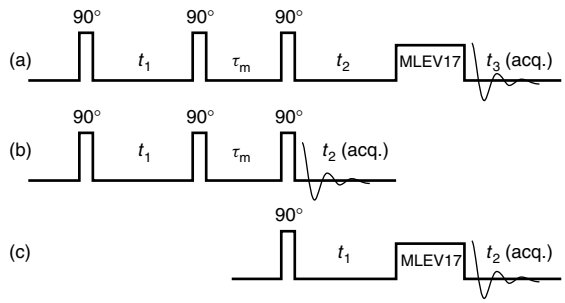

Figure 24.2. (a) Pulse sequence for a 3D NOESY–TOCSY experiment, constructed from (b) a 2D NOE experiment, and (c) a TOCSY experiment with a MLEV-17 mixing sequence.

In 3D experiments using TOCSY, NOESY, and ROESY mixing periods the magnetization is transferred not to one but to a number of other spins. Therefore, the J or NOE interactions can be observed at a number of 3D cross peaks. A coincidental overlap at one 3D cross peak can then be overcome by another nonoverlapping one. However, the disadvantages of such an approach are an increase in

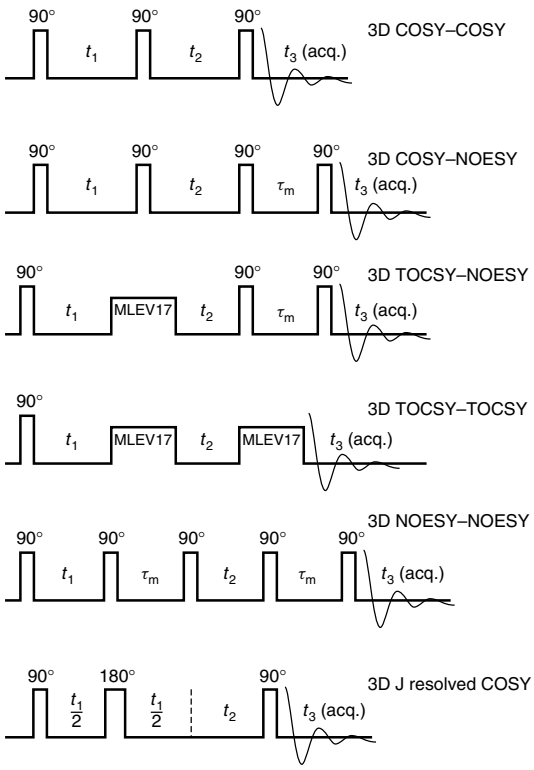

Figure 24.3. Pulse sequences for homonuclear 3D experiments.

complexity of the 3D spectra and a reduction of signal intensity by dilution. 3D spectra which use COSY-like relays, where magnetization is transferred to one other nucleus only, lead to spectra which are much more amenable for analysis. However, for protons the ^{3}J(H,H) coupling, which forms the basis for the COSY magnetization transfer, is relatively weak, and the necessary development of antiphase magnetization during the evolution and acquisition periods can take a long time compared with the T_2 relaxation time. This makes 3D experiments involving a proton–proton COSY transfer insensitive for biomolecules with a short T_2, and the long sampling of the t_1 or t_2 evolution periods may create excessively long recording times. The favorable J magnetization transfer induced by the HOHAHA effect is much more suitable for homonuclear 3D experiments of biomolecules. For large (>20 kDa) biomolecules the HOHAHA transfer can also become weak. In order to avoid complex analysis the selectivity of a relayed HOHAHA or a relayed NOE transfer may be optimized by choosing a relatively short mixing time. Other suitable building blocks for homonuclear 3D experiments of biomolecules are NOESY (or EXSY) and ROESY mixing periods.

24.5 SELECTIVE AND NONSELECTIVE HOMONUCLEAR 3D NMR

Since both the t_1 and t_2 domains of a 3D experiment (see Figure 24.2) have to be incremented independently, a large number of FIDs are recorded in order to obtain a sufficiently high resolution for these two domains. In principle, this could lead to long measuring times and to practical problems in handling large data sets.

Reduction of measuring time, the amount of collected data or a need for high digitization in a selected spectral area may require that the frequency sampling in the t_1 and t_2 domains is limited by means of using semiselective rf pulses which excite only a small portion of the NMR spectrum.[5–7] In this way one zooms in, as it were, onto a part of the complete 3D spectrum. Most of the early examples of homonuclear 3D experiments were semiselective: the semiselective COSY–COSY,[5,6] the semiselective NOESY–COSY,[6] and the semiselective NOESY–TOCSY.[7,36,37] The 3D J-resolved experiments[3,4] fall in a slightly different category, since they do not correlate chemical shifts across all mixing periods, but here also the recording time is relatively short. As in 2D J-resolved spectroscopy the aim of such experiments is the separation of chemical shifts and scalar (or dipolar) interactions, which may require a very different digitization.

In the nonselective 3D NMR experiments,[8] only hard pulses are used for the t_1 and t_2 domain, which allows for a complete sampling of all frequencies in the three dimensions. Although prolonged measuring times can be anticipated, some gain is obtained through the relative simplicity of the rf pulse sequences which makes short phase cycling schemes possible. In fact, most of the nonselective homonuclear 3D NMR experiments can be carried out within 2–5 days.

In terms of analysis, however, the semiselective and nonselective 3D NMR techniques are similar.

24.6 PRINCIPLES OF HOMONUCLEAR 3D SPECTROSCOPY

The 3D NOESY–TOCSY spectrum recorded with the pulse scheme of Figure 24.2 and obtained after 3D Fourier transformation of the FIDs can be schematically presented as a cube with three frequency axes, f_1, f_2, and f_3. In a 3D spectrum obtained in this way, a body diagonal ($f_1 = f_2 = f_3$) can be identified, which contains magnetization that was not transferred during any of the mixing periods. Additionally, intensity accumulates on the three cross-diagonal planes, which is shown in Figure 24.4. In the case of the 3D NOESY–TOCSY experiment, the plane $f_2 = f_3$ (NOE plane) contains magnetization transferred only during the first (NOE) mixing period, whereas the plane $f_1 = f_2$ (TOCSY or HOHAHA plane) contains magnetization transferred during the second (HOHAHA) mixing period. Finally, the plane $f_1 = f_3$ (back-transfer plane) contains magnetization that was transferred during the first (NOE) mixing period from proton *a* to proton *b* and then back to proton *a* during the second (HOHAHA) mixing period. For the analysis of 3D NMR spectra, cross sections perpendicular to one of the frequency axes can be used. Figure 24.5 shows an f_1–f_2 plane (which is perpendicular to the f_3 axis). The three diagonal planes of Figure 24.4 intersect this plane at the three lines indicated as NOE (or N), HOHAHA (or H) and back-transfer (or B) lines. These lines all share one point on the body diagonal of the spectrum.

Cross peaks that are present on the NOE and HOHAHA lines in the cross section taken at $f_3 = f_a$ represent single step magnetization transfer (by NOE and HOHAHA, respectively) to a proton *a*. Hence, the 3D

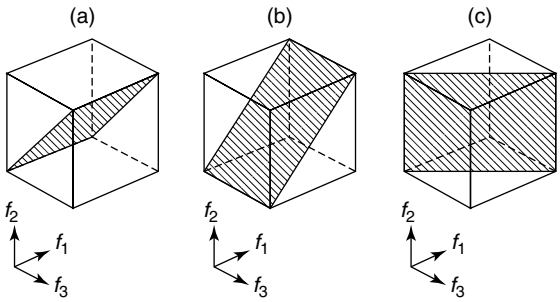

Figure 24.4. Cross-diagonal planes in a 3D NOESY–TOCSY spectrum: (a) NOE plane, (b) HOHAHA or TOCSY plane, and (c) back-transfer plane.

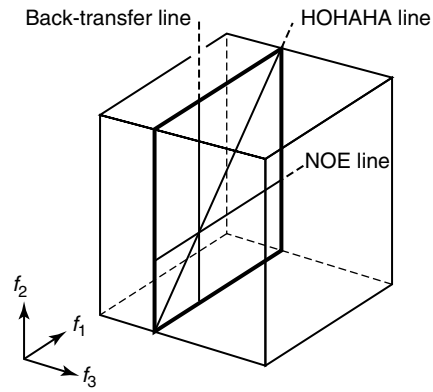

Figure 24.5. Schematic representation of an f_1–f_2 plane, perpendicular to the f_3 axis. The NOE, HOHAHA and back-transfer lines constitute the intersection with the three planes indicated in Figure 24.4.

NOESY–TOCSY spectrum contains the information that is present in traditional 2D NOESY and TOCSY spectra as a subset. All cross peaks outside the NOE and HOHAHA planes are due to double magnetization transfer. The double magnetization transfer that gives rise to peaks in the back-transfer plane is unique for homonuclear 3D experiments, since both mixing periods cover the same spectral frequencies. The closest 2D analogues of 3D NOESY–TOCSY experiments are relayed NOESY experiments[25,26] 2D TOCSY–NOESY,[27] and 2D ROESY–TOCSY and TOCSY–ROESY.[29] The information content of such spectra is present in the 3D spectrum as a projection onto the f_1–f_3 groundplane. However, since the cross peaks are labeled by three different frequencies, fewer ambiguities will arise in a 3D spectrum.

Figure 24.6 shows the nonselective 3D NOESY–TOCSY spectrum of a 109 residue protein, parvalbumin, in ^1H_2O. The spectrum contains a large number of cross peaks. Most of the intensity accumulates on the body diagonal and the NOE and HOHAHA planes. Less intensity accumulates on the back-transfer plane, because the associated magnetization must have gone through a double transfer. Intensities at positions ($f_1 \neq f_2 \neq f_3$), i.e. not on the three diagonal planes, correspond to magnetization which was transferred during both mixing periods. Figure 24.7 shows a contour plot of the NOE plane of the same 3D spectrum. This plot is very similar to a contour plot of the NOESY spectrum of this protein and indicates the need to increase the resolution for proteins of this size by

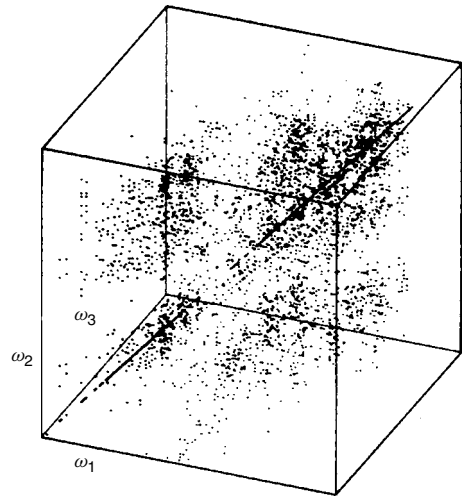

Figure 24.6. 3D NOESY–TOCSY spectrum of a 109-residue protein in ^1H_2O. The spectrum shows local intensity maxima for most cross peaks. The data set was recorded in 171 h at 500 MHz using an eight-scan phase cycle, as described by Vuister *et al.*[8] The NOE mixing time was 150 ms and the HOHAHA mixing time was 47 ms. The data were processed to a resolution of $256 \times 256 \times 256$. The sample contained 8.7 mM pike parvalbumin at pH = 4.1, 315 K, 10% D_2O.[8] (Reproduced by permission from Vuister *et al.*[8])

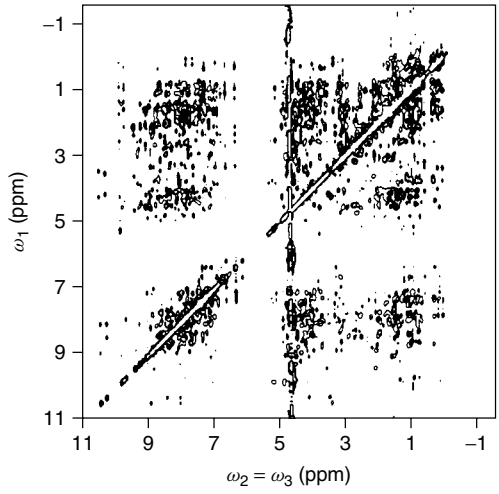

Figure 24.7. NOE plane of a 3D NOESY–TOCSY spectrum of the 109-residue protein of Figure 24.6. (Reproduced by permission from Vuister *et al.*[8])

using a third domain. Similarly, the HOHAHA plane resembles a TOCSY spectrum.

The analysis of 3D spectra can be accomplished in planes perpendicular to any axis of the 3D spectrum. In Figure 24.8(a) the flow of magnetization is sketched as observed in an f_1–f_2 plane of a 3D NOESY–TOCSY experiment. A cross peak at (f_a, f_b, f_c) indicates that magnetization started on a nucleus with frequency f_a was transferred by NOE to a nucleus with frequency f_b and was then transferred by isotropic mixing to a nucleus at f_c on the diagonal. Figure 24.8(b) shows the same flow in an f_2–f_3 plane, but now the magnetization originates from the diagonal. Finally Figure 24.8(c) shows this flow in an f_1–f_3 plane. The flow in a TOCSY–NOESY spectrum goes in the opposite direction, and the same planes can be constructed for the equivalent cross peak (f_c, f_b, f_a). Figure 24.8(d), 24.8(e) and 24.8(f) show the equivalence of the f_2–f_3, f_1–f_2, and f_1–f_3 planes of a 3D TOCSY–NOESY spectrum with that of the f_1–f_2, f_2–f_3, and f_3–f_1 planes of a 3D NOESY–TOCSY spectrum, respectively. Only the flow, as indicated by the arrows, is inverted, while the appearance of the spectrum is the same.

The cross peaks in 3D spectra reflect connectivities between the spins. To describe the connectivities the C notation can be used: $C[M_1, M_2]_{abc}$ (i, j, k) or shorthand C_{abc} (i, j, k) means that magnetization of proton a in residue i is interacting via mixing step M_1 with proton b of residue i and next via mixing step M_2 to proton c of residue k. Thus, 3D NOESY–TOCSY and 3D TOCSY–NOESY spectra contain the same connectivity information: a $C[NOE, J]_{abc}$ (i, j, j) pathway is equivalent to a $C[J, NOE]_{cba}$ (j, j, i) pathway. Both represent the same combination of interactions. Experimentally, however, differences in t_1 and t_2 noise and in domain resolution make it quite different, whether a $C_{NN\alpha}$ ($i + 1$, i, i) connectivity is observed in an f_1–f_2 plane at f_3 of the α proton (such as in 3D NOESY–TOCSY) or at f_3 of the NH proton (as in 3D TOCSY–NOESY).

24.7 PRACTICAL ASPECTS

24.7.1 Sensitivity

For 3D spectra a better signal-to-noise ratio is required than that of the 2D analogs, since the aim of 3D experiments is the observation of weak double magnetization transfers. Therefore, 3D techniques

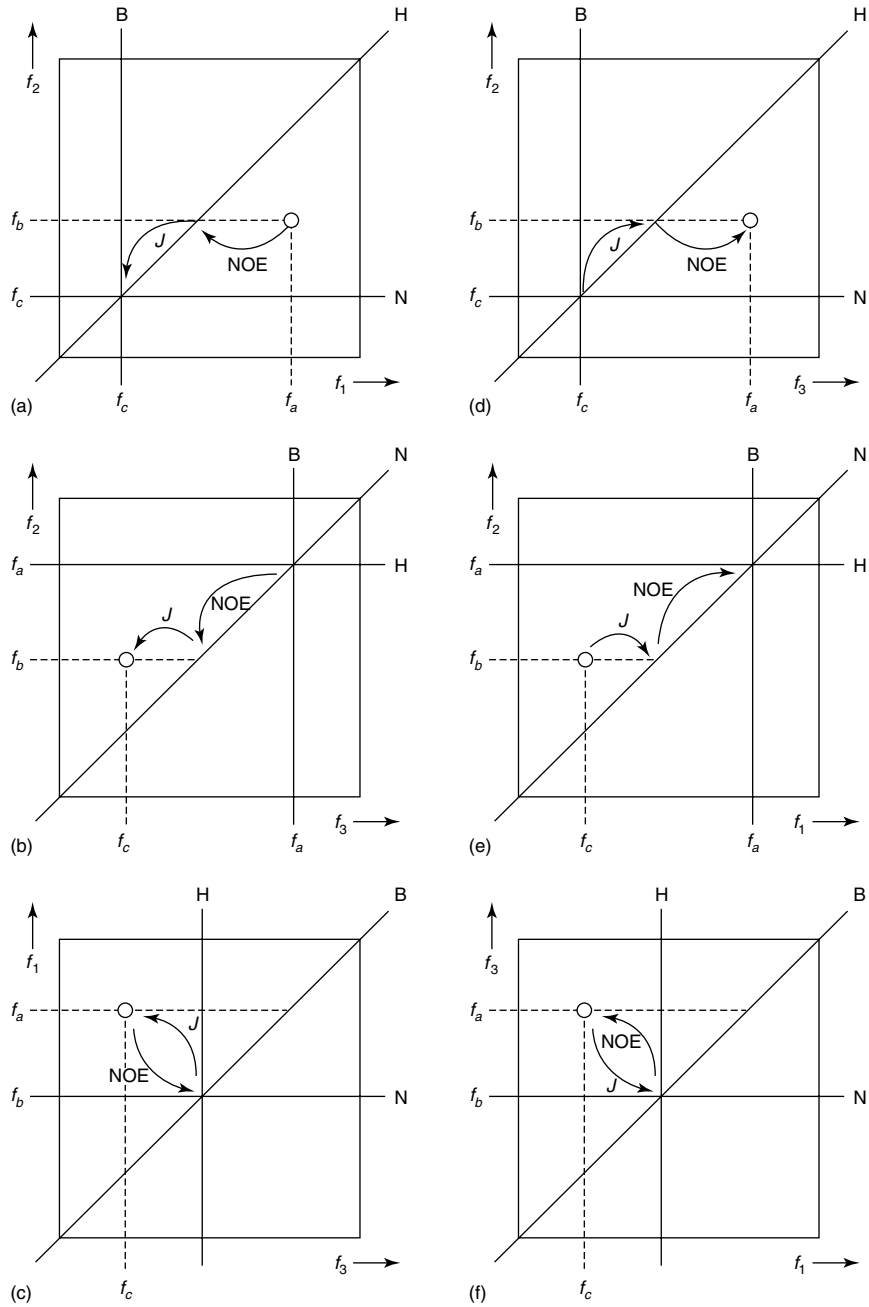

Figure 24.8. Flow of magnetization for a cross peak (f_a, f_b, f_c) in a 3D NOESY–TOCSY spectrum and the equivalent cross peak (f_c, f_b, f_a) in a 3D TOCSY–NOESY spectrum. (a)–(c) The f_1–f_2, f_2–f_3, and the f_1–f_3 planes of a 3D NOESY–TOCSY spectrum. (d)–(f) The f_2–f_3, f_1–f_2, and the f_1–f_3 planes of a 3D TOCSY–NOESY spectrum. The lines indicated by N, H, and B are the cross-diagonal NOE, HOHAHA (or TOCSY), and back-transfer lines, respectively. Only the flow of magnetization in the two spectra reverses; the appearance of both spectra is the same.

should only be applied in case of overlap in optimally recorded 2D spectra.

The sensitivity of a 3D experiment is determined by the efficiency of magnetization transfer in the mixing periods, by T_2 relaxation during the evolution and acquisition periods, and the method of selecting the evolved magnetization. As in 2D spectroscopy most mixing periods select only the x or y component of the magnetization from the previous evolution period, and by phase cycling the other term is removed. This leads to the loss of half of the magnetization and half of the noise power. Therefore, as pointed out by Bax and Grzesiek,[20] each addition of dimensionality may lead to a signal-to-noise reduction by $1/\sqrt{2}$. This loss in the signal-to-noise ratio can, however, be avoided by retaining both orthogonal magnetization components across the mixing periods (see Cavanagh and Rance[38] for a review). This method has been applied to 3D NOESY–TOCSY.[39] A drawback may be, however, an increase in experiment time due to additional phase cycling in order to obtain phase-sensitive spectra.

In 3D spectrocopy the signal accumulates independently in all domains. By minimizing the length of the evolution periods, loss of sensitivity due to T_2 relaxation can be avoided. The length of the evolution periods should be only so long that overlap of cross peaks is avoided, or as required for the further analysis of the 3D spectra. Since there is a lower chance of overlap in 3D than in 2D spectra the evolution periods can clearly be shorter in 3D spectra. With the crowded spectra of biomolecules, however, it is difficult to predict which resolution is finally needed until the analysis is completed. As a guideline it is noted that sampling with the evolution periods beyond $0.9T_2$ is only to increase resolution, while sampling below $0.9T_2$ will add signal to the multidimensional cross peaks. The sensitivity of the NOE and HOHAHA planes of an optimally recorded 3D NOESY–TOCSY spectrum will be similar to that of the two 2D counterparts recorded together in the same total time. However, the aim of a 3D experiment is clearly the observation of double magnetization transfer, and the corresponding cross peaks will be much weaker.

For good sensitivity of multidimensional experiments it is extremely important to optimize the transfer efficiencies of the mixing periods. For TOCSY, various improvements have been published, compensating relaxation by "clean" TOCSY pulse sequences[40] or increasing sensitivity by orthogonal magnetization transfer, as discussed above. For ROESY, potential J transfer should be minimized (see Chapter 20).[35] For NOESY no fundamental optimizations are possible, but accurate and homogeneous 90° rf pulses will enhance the transfer. In all cases the transfer efficiencies may be optimized by adapting the length of the mixing period. Since the cross-peak intensity in 3D spectroscopy is proportional to the product of the constituent 2D transfer efficiencies, an optimal 2D mixing time will also be the optimum for three dimensions.

Another important factor for sensitivity is the number of rf pulses in combination with pulse imperfections, i.e. inaccurate flip angles or B_1 inhomogeneities. Generally, phase cycles of 2D and 3D experiments are set up so that only coherences are selected which pass the sequence assuming ideal 90° and 180° pulses and that coherences created by the imperfections are suppressed. Since most homonuclear 3D sequences contain only a few rf pulses or a self-compensated isotropic mixing period, only a small amount of magnetization is lost in this way.

However, in many cases the actual sensitivity is less favorable due to t_1 and t_2 noise caused by instrument instabilities. Such instabilities are present in 2D spectroscopy as well, but the 3D technique may sample additional instabilities due to the length of the experiment and the wish to minimize recording time. On some NMR instruments undefined delays may be introduced between the FIDs. A constant steady state magnetization may be maintained by a buffered acquisition method or by steady state pulses. Fluctuations in the extent of sample heating due to the pulse sequence are more difficult to avoid.

24.7.2 Phase Cycling and Recording Time

Both phase cycling or field gradients can be used for selecting the coherence transfer pathway in 3D experiments. Since the gradients do the selection in single experiments, use of gradients is preferable for 3D spectroscopy. Thus, the NOE effect can be selected by a single gradient pulse in the NOE mixing period.[31] However, the number of phase cycling steps can also be minimized in 3D spectroscopy. For large biomolecules the phase cycling to select NOE mixing can be short, since most undesirable coherences have decayed at the end of the NOE mixing time. Suppression of single quantum coherences is normally sufficient and can

be accomplished by two phase steps. The HOHAHA mixing requires no selection of coherence level at all, if a "clean" MLEV sequence is used.[40] Axial peaks due to T_1 relaxation can be suppressed by inversion of the first 90° rf pulse, which will double the phase cycle. Inaccurate 90° or 180° rf pulses may lead, however, to an axial plane at the f_1–f_3 ground plane of a 3D spectrum, which can be removed by inverting all pulses before the t_2 period. In order to separate positive and negative frequencies in the t_1 and t_2 domains, either a time proportional phase increment (TPPI) or a States–TPPI sampling scheme should be used, which will put potential axial peaks at the sides of the 3D cube. Homonuclear 3D spectroscopy with minimal phase cycling has been demonstrated for 3D NOESY–NOESY[41] and for 3D TOCSY–NOESY.[42] In practice, 3D TOCSY–TOCSY and gradient enhanced 3D TOCSY–NOESY with axial peak suppression in t_1 will have a minimal two-step phase cycle inverting only the very first rf pulse. Without gradients the minimal phase cycling for 3D TOCSY–NOESY becomes four and for 3D NOESY–NOESY already eight, while inclusion of axial plane correction brings this to 8 and 16, respectively.

NMR receiver imperfections may require additional phase cycling in order to remove dc bias and quad-image artifacts, but they can be mixed into the phase cycle for coherence selection. Thus, depending on the level of artifact suppression needed, phase cycles of 1–6 scans can be used. Typically, 128–256 independent t_1 and t_2 increments are used to sample the corresponding domains, with an acquisition size of 512–1024 words. In order to reduce measuring time, the relaxation delay between each scan is set to a value close to the T_1 relaxation time of the biomolecule, which results in some saturation. In this fashion, the repetition rate per scan is about 1 s, and a typical $160 \times 256 \times 1024$ 3D TOCSY–NOESY experiment takes between 46 h for a four-scan and 182 h for a 16-scan version and will create 42 Mwords of data.

24.7.3 Processing

The heavily truncated interferograms in the t_1 and t_2 periods of 3D datasets are in principle not suitable for frequency analysis by fast Fourier transforms. Apodization functions such as the Hamming or Kaiser windows vastly decrease the amount of "ripple" (cf. Ernst *et al.*[2]). A better approach is frequency analysis by parametric methods based on linear prediction[43–45] and by the maximum entropy or Bayesian methods,[46] but these methods can be computationally expensive. A more modest but practical approach is the extension of the experimental data set by linear prediction, followed by window multiplication and a fast Fourier transform.[47] Phasing parameters for the evolution periods can either be calculated from initial delay values and rf pulse widths[48] or estimated by visual inspection of the data. After the Fourier transform the 3D spectrum can be baseline corrected in all domains by a variety of methods.[49,50] Offsets and baseline distortions in the f_1 and f_2 domains can, however, already be minimized by data sampling techniques.[51,52]

For the manual analysis of 3D spectra, contour plots can be produced for all cross sections that contain cross peaks. This approach may be sufficient for settling overlap in crowded 2D spectra. Since bookkeeping of all peaks in a 3D spectrum can be cumbersome, analysis with a workstation is to be preferred. Programs have been developed that can assist the manual analysis of such spectra.[53–56] A step further is the automatic or semiautomatic analysis of patterns of correlated cross peaks, e.g. for assigning 3D proton spectra.[54,57,58] The input of such programs may require further processing of the spectra, e.g. searches of local maxima and peak boundaries, peak decomposition, and determination of intensities.

24.8 APPLICATIONS

24.8.1 3D J-Resolved Spectroscopy

The 3D J-resolved experiment can be visualized as a 2D J-resolved experiment in which the acquisition period has been replaced by the evolution period, mixing period, and acquisition period of a second 2D experiment. Both COSY[3,4,59] and NOESY[60] have been suggested for this second experiment. Such 3D J-resolved spectra can become useful when overlap interferes with the analysis of multiplet patterns in a 2D J-resolved spectrum. A drawback of J-resolved spectroscopy (see Chapter 11) for measuring J-couplings as compared with E.COSY techniques (see Chapter 14)[61] is that the multiplet pattern is not simplified, but remains at full complexity. This explains the limited application of the method for high-resolution studies of biomolecules. Related 3D

experiments in solid state NMR for separating chemical shift and dipolar interactions have found more extensive use.[62,63] The 3D J-resolved method demonstrated, however, the feasibility of 3D NMR and started the development of a large number of other 3D techniques.

24.8.2 3D TOCSY–NOESY and 3D NOESY–TOCSY Spectroscopy

For most biomolecular studies both the J-coupling and the NOE interaction must be measured. Such interactions can be obtained by separate NOESY and COSY or TOCSY experiments, but it is logical to combine both into one 3D experiment in which one mixing period contains the NOE effect and the other the J-coupling. Two types of homonuclear experiments can be envisaged: 3D NOE–J and 3D J–NOE. The first implementation was shown by Griesinger *et al*.[6] in a semiselective 3D NOESY–COSY experiment. However, for larger biomolecules the J effect is transferred much more efficiently by a HOHAHA mixing period, as was demonstrated by Oschkinat *et al*.[7] in a semiselective 3D NOESY–TOCSY experiment of a 46-residue protein. Shortly after, it was shown that complete nonselective 3D NOESY–TOCSY experiments of proteins can also be executed in a reasonable time.[8] Later improvements used "clean" MLEV sequences[37,64,65] and orthogonal isotropic mixing[39] to enhance the amount of transferred magnetization.

24.8.3 Observation of Sequential NOEs in Proteins

The combined observation of J-couplings and NOE interactions in 3D NOESY–TOCSY spectra makes it possible to assign the proton resonances in the protein spectrum by a similar sequential assignment strategy as developed by Wüthrich and his co-workers[1] for 2D spectra. In the 2D approach, the spin systems of the protons belonging to one amino acid residue are identified by exhaustively analyzing the through-bond proton–proton connectivities in COSY and TOCSY spectra. The sequentially neighboring amino acid spin systems are then identified by observation of the sequential d_{NN}, $d_{\alpha N}$ and $d_{\beta N}$ connectivities in 2D NOE spectra. Starting at a unique spin system or by matching unique di- and tripeptide sequences on the complete protein sequence, the spin systems can be assigned to specific amino acids. In a simplified view, the spin system analysis can be reduced to observing αN connectivities between the J-coupled α and NH protons of each amino acid residue, while the sequential assignment is based (among others) on αN connectivities between neighbors. In 3D NOESY–TOCSY and 3D TOCSY–NOESY experiments, we can measure both types of connectivity simultaneously in one $C[NOE,J]_{N\alpha N}(i + 1, i, i)$ connectivity. In fact, two types of NαN connectivities exist: sequential $C_{N\alpha N}(i + 1, i, i)$ and intraresidue $C_{N\alpha N}(i, i, i)$ connectivities. Both connectivities can be observed in the scheme shown in Figure 24.9. The intraresidue $C_{N\alpha N}(i, i, i)$ connectivity of residue i will be found on the back-transfer line of an f_1–f_2 plane, whereas the sequential $C_{N\alpha N}(i + 1, i, i)$ connectivity to residue $(i - 1)$ will be found on a line parallel to the NOE line through the intraresidue $C_{N\alpha N}(i, i, i)$

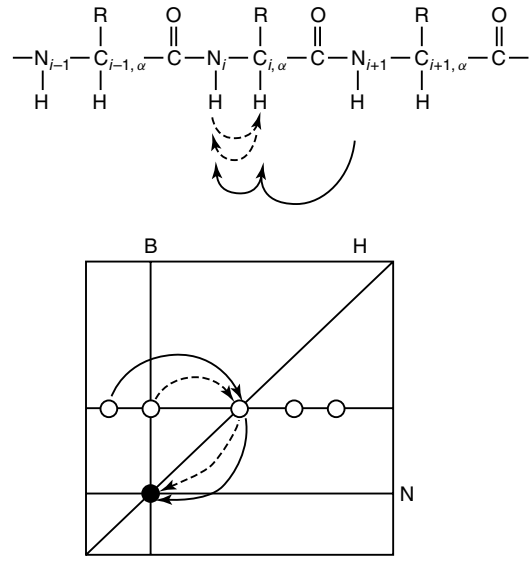

Figure 24.9. Sequential and intraresidue $C_{N\alpha N}$ connectivities in an f_1–f_2 plane of a 3D NOESY–TOCSY spectrum. The lines indicated by N, H, and B are the cross diagonal NOE, HOHAHA (or TOCSY), and back-transfer lines, respectively. The two dotted arrows starting at a back-transfer cross peak indicate the intraresidue $C_{N\alpha N}(i, i, i)$ connectivity, where the first arrow represents the NOE transfer from N to α and the second one the J transfer from α back to N. The two solid arrows show the interresidue $C_{N\alpha N}(i + 1, i, i)$ connectivity.

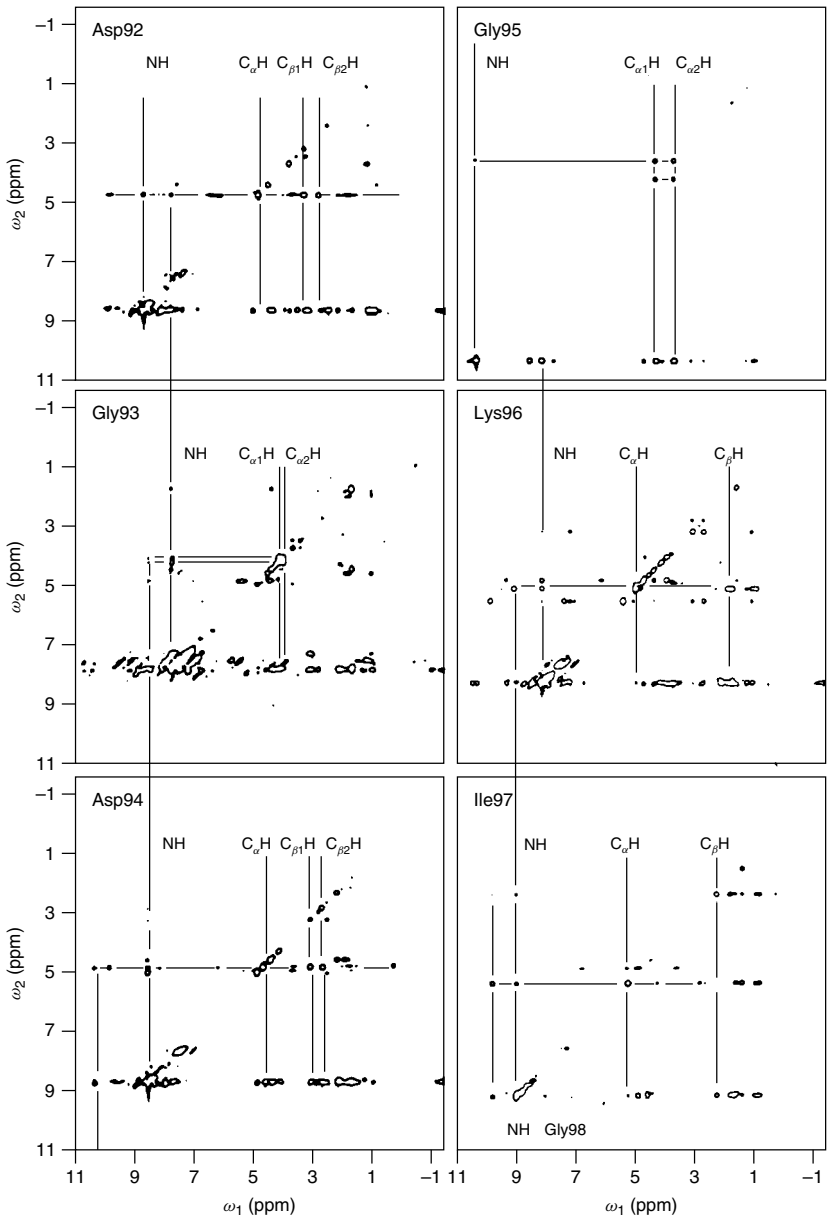

Figure 24.10. Sequential walk through $f_1 - f_2$ planes in the NH region of the 3D NOESY–TOCSY spectrum of parvalbumin for f_3 frequencies of NH(Asp92) to NH(Ile97), taken from Vuister *et al.*[8] The spin system is indicated by vertical lines for each plane. The NOEs with the C-α atom can be found on the horizontal line parallel to the NOE line at the C-α resonance frequency. A back-transfer peak, $C_{N\alpha N}(i, i, i)$, is found at the crossing with the vertical NH line. The other cross peaks on this horizontal line in the NH region represent potential sequential cross peaks $C_{N\alpha N}(i + 1, i, i)$. The vertical line connecting to the next $f_1 - f_2$ plane defines the NH frequency of the neighboring residue. The number of choices for sequential connectivities is significantly reduced compared with that observed in 2D spectra. Note that at Gly95 the sequential $C_{N\alpha N}$ $(i + 1, i, i)$ connectivity is lacking, but that in this case use has been made of the single-step d_{NN} connectivity on the NOE line. (Reproduced by permission from Vuister *et al.*[8])

connectivity. This then defines the NH f_3 frequency for the next f_1–f_2 plane, where we can repeat the search for both connectivities. An example of such a sequential assignment is given in Figure 24.10 for the 3D NOESY–TOCSY spectrum of pike parvalbumin from Asp92 to Ile97.

Complete descriptions of the sequential assignment strategy using 3D NOESY–TOCSY or 3D TOCSY–NOESY spectra were given by Vuister *et al*.[66] and by Oschkinat *et al*.[67] A full analysis of all possible 3D sequential connectivities in proteins was given, and estimates of the relative intensities of cross peaks corresponding to such connectivities for α-helical and β-sheet conformations, as summarized in Table 24.1 (for α- and N-protons only). Thus, by searching the 3D spectrum for such connectivities it is possible to analyze the secondary structure of the protein.

The method has been applied to the 109 amino acid residue protein parvalbumin. Most of the sequential backbone cross peaks of this protein were observed[68] in a single 3D TOCSY–NOESY spectrum of parvalbumin. The assignment based on these 3D data corresponds completely with a previous one using extensive 2D data. Even some novel NOEs, hidden due to overlap in the 2D spectra of parvalbumin, could be identified. Similar results have been obtained for α-purothionin,[37] bovine pancreas trypsin inhibitor (BPTI),[67] the 113-residue protein aponeocarzinostatin,[69] a 90-residue phospholipid transfer protein,[70] a 137-residue flavodoxin,[65] the 128-residue blue copper protein azurin,[71] the 153-residue interleukin-4,[21] and the monomeric 143-residue heme protein leghemoglobin.[72] In most cases the analysis of the homonuclear 3D data led to additions or corrections in previously established assignments. The assignment for one residue was corrected for α-purothionin. Parvalbumin was shown to contain one amino acid residue more than expected on the basis of the amino acid sequence. For flavodoxin, 15 additional residues were identified from the 3D spectra. For neocarzinostatin it was possible to correct inconsistent assignments from three previous publications.

It is clear that the combination of NOE transfer and isotropic mixing in one 3D experiment is very useful in sequential assignment procedures of protein NMR spectra. Since the information is contained in one data set, these procedures may be better suited for automation than methods which rely on matching two different NOESY and TOCSY spectra. Furthermore, the increased resolution and the presence of the two-step connectivities will reduce overlap in spectra of larger biomolecules. Semiautomated approaches for analyzing 3D NOESY–TOCSY spectra of proteins have been demonstrated by Oschkinat *et al*.[57,58] and Kleywegt *et al*.[54] In this latter procedure, sets of J-coupled resonances are obtained from a peak list of the 3D spectrum. These sets are then ranked as possible spin systems using chemical shift rules and the sets are ordered using sequential 3D connectivities. By matching long stretches of such sequentially linked spin systems versus the amino acid sequence it is possible to assign almost all residues of parvalbumin.[54]

In a semiautomatic procedure the analysis of 3D spectra can take place in f_1–f_2, f_2–f_3, or f_1–f_3 planes: the relationships among the cross peaks in different planes are established by the rules within the program. In an interactive analysis, especially on paper, patterns are more easily recognized in a single plot. The analysis of 3D TOCSY–NOESY and 3D NOESY–TOCSY spectra in f_1–f_3 planes has been found to be convenient, since the pattern of HOHAHA related cross peaks and the NOE relationship of this pattern with other resonances can be observed in one plane. Such planes are useful for identifying amino acid spin systems and a sequential assignment strategy mainly using f_1–f_3 planes has been outlined.[42,65]

Of course, it is not necessary to use just one 3D TOCSY–NOESY spectrum for assigning the resonances. A pragmatic approach uses 2D TOCSY and NOESY spectra for identifying the interactions between nonoverlapping resonances, whereas ambiguities are sorted out using the 3D spectra. Such procedures have been used for neocarzinostatin,[69] leghemoglobin,[72] procolipase,[73] the DNA binding domains of LexA repressor,[74] and the transcription elongation factor TFIIS.[75] Also for interleukin-4[21] and for azurin,[71] 3D TOCSY–NOESY and 3D NOESY–(^{15}N, ^{1}H)–HMQC were used together to resolve ambiguities in the assignments.

24.8.4 Identification of Spin Systems using 3D TOCSY–TOCSY Spectroscopy

An essential step for the sequential analysis of protein NMR spectra is the identification of spin systems. It has been demonstrated that 3D TOCSY–TOCSY spectroscopy can be of great help for deciphering spin

Table 24.1. Sequential connectivities in 2D and 3D NMR[a]

	α-helix	β-sheet
2D NOE or NOE plane		
$d_{\alpha N}$	w	s
d_{NN}	m	a
3D NOESY–TOCSY		
$d_{\alpha N}$ $C_{N\alpha N}(i+1,i,i)$	a–w	s
$C_{\alpha N\alpha}(i-1,i,i)$	a–w	s
d_{NN} $C_{NN\alpha}(i+1,i,i)$	m	a–w
$C_{NN\alpha}(i-1,i,i)$	m	a–w

[a]Cross peak intensities: s, strong; m, medium; w, weak or a, absent. The estimates for the intensities in the 2D NOE spectra are taken from Wüthrich,[1] those for the 3D NOESY–TOCSY spectra are calculated as described by Vuister *et al.*[66]

systems.[76] The analysis of a 3D TOCSY–TOCSY spectrum is more straightforward than that of a 3D TOCSY–NOESY spectrum, since each 3D cross peak already defines three frequencies of the spin system. Similarly as in 3D TOCSY–NOESY spectra, it is relatively easy to recognize in the f_1–f_3 planes the 3D cross peaks belonging to one spin system, even in the case of overlap at the f_2 frequency. Oschkinat *et al.*[58] have proposed a strategy for automated assignment of proteins, where the spin systems would be identified using a 3D TOCSY–TOCSY spectrum and the sequential connectivities between the spin systems are obtained from a 3D TOCSY–NOESY spectrum. 3D TOCSY–TOCSY spectra can be very useful in those cases where strong overlap prohibits the analysis of spin systems but where efficient HOHAHA transfer is still present.

24.8.5 Analysis of 3D NOESY–NOESY Spectra

For larger proteins it becomes more difficult to establish the proton–proton J-coupling via COSY and HOHAHA transfer steps. A 3D technique, where both mixing periods are due to cross relaxation, is in principle not limited by molecular weight. Suitable mixing periods are NOE or ROE. Thus, 3D NOESY–NOESY spectroscopy was proposed, where a NOE is now relayed by NOE to another nucleus.[11] However, since the relay can be to any neighboring nucleus, the analysis of 3D NOESY–NOESY spectra can be complex. Furthermore, since in general the NOE is weak and the relay can be to several other nuclei, a relatively low sensitivity for the 3D NOESY–NOESY could be expected. Nevertheless, 3D NOESY–NOESY spectra of good quality have been presented.[41,77–79] For proteins it has been demonstrated that the amide protons show connectivity patterns very similar to 3D NOESY–TOCSY spectra.[77] A statistical analysis of expected connectivities in 3D NOESY–NOESY spectra for 28 crystal protein structures shows that patterns of highly correlated cross peaks exist, suggesting that assignments for proteins could be based largely on NOE data.[80] A very complete analysis of sequential and medium range connectivities has been made for the 3D NOESY–NOESY spectrum of parvalbumin.[41,78] For the 109-residue parvalbumin the HOHAHA transfer is generally more efficient than the NOE transfer, thus the number of sequential and medium range connectivities in the 3D NOESY–NOESY spectrum is slightly less than that of a 3D TOCSY–NOESY spectrum. For proteins with a less efficient HOHAHA transfer, however, 3D NOESY–NOESY may perform better.

24.8.6 Structural Studies of Proteins

Stretches of sequential and medium range 3D connectivities can be used as indicators for α-helical, β-sheet, or turn-like structures. Thus, for the proteins parvalbumin[68] and aponeocarzinostatin[69] it was demonstrated that most of the secondary structure assignments found in 2D NOE spectra can be obtained from a 3D TOCSY–NOESY spectrum, but with fewer ambiguities. The secondary structures of a phospholipid transfer protein[70] and of leghemoglobin[72] are based on a combination of homonuclear 2D and 3D data. For ferrocytochrome c_{553} several crucial long range NOEs could be established from 3D TOCSY–NOESY spectra.[81] Similarly, many NOE restraints used for the structure determinations of procolipase[73] and the DNA binding domain of LexA repressor[74] were obtained with help from 3D TOCSY–NOESY data.

Long-range NOEs can also be observed by 3D NOESY–NOESY. Thus, 3D NOESY–NOESY data resolved crucial long range connectivities for the structure determination of the DNA binding domain of LexA repressor.[74] The analysis of 3D NOESY–NOESY spectra is complex, since a large

number of cross peaks can be expected and the magnetization transfer is not limited to spin systems. The analysis improves by comparing patterns of 3D cross peaks. For example, if for spin B a characteristic pattern of cross peaks {(A, B, P), (A, B, Q), and (A, B, R)} has been observed, the 3D NOESY–NOESY spectrum can be searched systematically for the patterns {(C, B, P), (C, B, Q), and (C, B, R)} and {(P, B, C), (Q, B, C), and (R, B, C)}. If the pattern at the row defined by (f_1, f_2) = (A, B) was observed virtually without overlap, this search is effectively a convolution of the 3D spectrum with this row. Visually, this pattern can be easily recognized in an f_1–f_3 plane. Next, one has to analyze the pattern at (f_1, f_2) = (B, C) in order to establish the nature of nucleus C. In this way the pattern of relayed intensities, which was unfavorable for an optimal signal-to-noise ratio of the 3D spectrum, turns out to be beneficial for pattern recognition. Once the 3D cross peaks have all been assigned, the intensities of the 3D cross peaks can be converted into constraints for structure refinement.

24.8.7 Distance Constraints from 3D Data

For structure refinement it is important to obtain as many distance constraints as possible.[1] For this, 3D spectra can be very useful, since they may resolve many ambiguities in the spectral interpretation of NOE data, and therefore lead to more restraints.[82] It is, however, also possible to use the 3D spectra directly for obtaining distance constraints. The 3D cross-peak intensity is proportional to the product of the two transfer efficiencies of the two mixing periods of a 3D experiment:

$$I_{ijk} \propto T_{ij} T_{jk} \tag{24.1}$$

Several approaches have been described for interpreting the 3D intensity. The ratio of the intensity of the cross peak C(A,B,C) of a 3D TOCSY–NOESY, or a 3D NOESY–NOESY spectrum and the intensity of the cross-diagonal cross peak C(A,B,B) defines the transfer efficiency T_{bc}:

$$I\{\mathrm{C(A,B,C)}\}/I\{\mathrm{C(A,B,B)}\} = T_{bc}/(1 - T_{bc}) \tag{24.2}$$

From this NOE transfer efficiency, T_{bc} distances can be obtained in a similar way as from regular 2D data. The relationship between NOE transfer efficiency and cross relaxation rates is

$$\boldsymbol{T} = \exp(-\tau_{\mathrm{m}} \boldsymbol{R}) \tag{24.3}$$

where $\boldsymbol{T}$ and $\boldsymbol{R}$ are the NOE transfer and cross-relaxation matrices, respectively, and τ_{m} the NOE mixing period. Generally, transfer efficiencies are compared with those of protons at known distances and the approximate relationship

$$T_{bc}/T_{de} = (r_{de}/r_{bc})^6 \tag{24.4}$$

is used. In the case of overlap at the cross-diagonal planes it is still possible to obtain the ratio of the cross peaks C(A,B,C) and C(A,B,F) which defines the ratio T_{bc}/T_{bf} and thus the ratio of the distances r_{bc}/r_{bf}.[83] If the distance r_{bf} is known, the distance r_{bc} can be derived.

A more quantitative approach uses the cross-peak intensities of a 3D NOESY–NOESY spectrum. The relationship between NOE and distance is only an approximate one, due to spin diffusion at longer NOE mixing times. Approximating this multiple-step NOE transfer to second order, the NOE intensity is equal to

$$T_{ij} = -R_{ij}\tau_{\mathrm{m}} + \sum R_{ik} R_{kj} \tau_{\mathrm{m}}^2 \ldots \tag{24.5}$$

The second term in equation (24.5) describes spin diffusion via other spins. The intensity of a cross peak in a 3D NOESY–NOESY spectrum is to a first approximation equal to

$$T_{ikj} = R_{ik} R_{kj} \tau_{\mathrm{m}}^2 \ldots \tag{24.6}$$

Thus the cross peaks in a 3D NOESY–NOESY spectrum define the contributions of the several spin diffusion paths via other nuclei.[11] Therefore the 3D NOESY–NOESY intensities can be used to obtain more accurate cross-relaxation rates between proton pairs, as has been shown by Kessler *et al.*[84] and Habazettl *et al.*[85]

The 3D NOESY–NOESY intensities can also be used as direct constraints for a structure refinement. This requires the calculation of the gradients of the 3D intensities with respect to the coordinates of the protons in a molecule. The gradient of a 3D NOESY–NOESY peak with a net transfer T_{ijk} can be written[86] as the sum of two terms containing the separate gradients of T_{ij} and T_{jk}:

$$\nabla T_{ijk} = T_{ij} \nabla T_{jk} + \nabla T_{ij} T_{jk} \tag{24.7}$$

The transfer efficiencies T_{ij} and T_{jk} can be obtained from relaxation matrix methods (cf. Bonvin *et al.*[87]), while the derivatives of the 2D efficiencies can be solved exactly[88] or be approximated.[89] equation (24.7) has been used to obtain 3D NOE restraining

potentials for use in restrained molecular dynamics calculations:[86,90,91]

$$V_{3D\,NOE} \sim \sum_{ijk} (T_{ijk} - T_{ijk}^{obs})^2 \qquad (24.8)$$

where T_{ijk} and T_{ijk}^{obs} are the calculated and observed transfer efficiencies, respectively. The minimization of the 3D NOE potential requires the calculation of ∇V_{3DNOE}. This can be accomplished by combining equations (24.7) and (24.8) as

$$\nabla V_{3D\,NOE} \sim \sum_{ijk} 2(T_{ijk} - T_{ijk}^{obs}) \times (T_{ij} \cdot \nabla T_{jk} + \nabla T_{ij} \cdot T_{jk}) \qquad (24.9)$$

It has been shown that the use of the 3D cross-peak intensities can lead to a better definition of the structures of proteins than the use of only 2D NOE data.

24.8.8 Protein Hydration Studies

Cross peaks in a NOESY spectrum at a line corresponding to the f_1 frequency of water can identify protons with a close proximity to water.[92] The overlap of proton signals on this line can be removed by transferring the magnetization in a second magnetization transfer step to a third nucleus. Thus, Otting *et al.*[93] have demonstrated the use of 3D NOESY–TOCSY and 3D ROESY–TOCSY for studies of protein hydration, whereas Holak *et al.*[94] have used 3D NOESY–NOESY. In contrast to 2D methods, where the NOEs with water protons are all observed on a single frequency axis, the f_2–f_3 planes of 3D spectra at the f_1 frequency of water reveal the protons interacting with water via cross peaks in a two-dimensional map. This reduces overlap and helps to assign the protons involved. The comparison of the sign and intensities of the cross peaks in the f_2–f_3 planes of the 3D NOESY–TOCSY and 3D ROESY–TOCSY spectra distinguishes NOE and exchange effects.

24.8.9 Homonuclear 3D NMR of Oligosaccharides

The small chemical shift dispersion of the sugar-skeleton protons of oligosaccharides poses a major problem for structural studies. It is often still possible to obtain assignments on the basis of 2D HOHAHA experiments by exploiting the chemical shift dispersion of the anomeric protons. However, the unique identification of NOEs involving protons in the bulk region between 3 and 4 ppm is very difficult. The resolution in the bulk region can be increased by the application of 3D NOESY–TOCSY techniques, which relay the magnetization from the bulk protons to the anomeric signals.[83,95]

An example is given in Figure 24.11, which shows the f_1–f_2 plane at the f_3 frequency of the Man-4 H-2 anomeric signal of a biantennary asparagine-linked oligosaccharide at 4.19 ppm. An interesting 3D cross peak is observed at the f_1 frequency of Man-3 H-2, which shows the presence of an NOE between Man-4 H-5 and Man-3 H-2. The existence of this NOE was the subject of considerable discussion in the literature, although it was settled later by deuteration studies (see Vuister *et al.*[95] for a discussion). This NOE effect is found directly in the 3D NOESY–TOCSY spectrum.

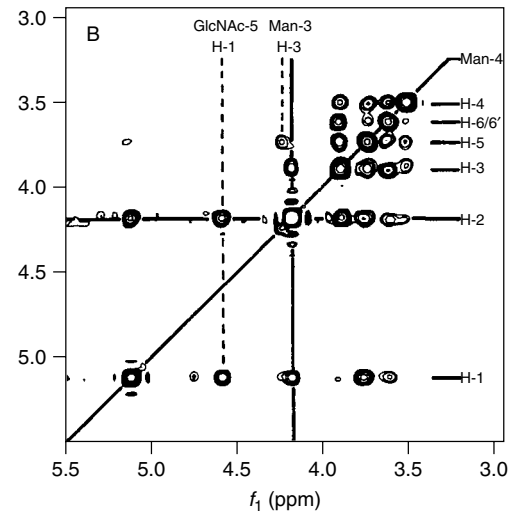

Figure 24.11. f_1–f_2 plane of the 3D NOESY–TOCSY spectrum of 20 mM biantennary oligosaccharide in D_2O at 304 K and pH = 7. The cross section shown is at the f_3 resonance position of Man-4 H-2 (4.19 ppm). The 144 × 144 × 1024 data set was recorded at 500 MHz in 63 h using eight scans. The NOE mixing time was 350 ms and the HOHAHA mixing time 94 ms. The spectrum was processed to a resolution of 256 × 256 × 512. (Adapted by permission from Vuister *et al.*[95])

24.8.10 Homonuclear 3D NMR of DNA and RNA Fragments

For the sequential assignment of DNA and RNA fragments it is necessary to correlate the NOEs of the aromatic protons of the nucleic acid bases with their own sugar protons and those of their neighbor. 3D TOCSY–NOESY spectra can be used for this purpose.[96,97] It turns out that even the very crowded 4′,5′,5″ region of DNA fragments now becomes accessible for analysis. Thus, 3D TOCSY–NOESY was used for a 15-residue DNA hairpin,[96] and 3D NOESY–TOCSY for a 31-residue pyrimidine–purine–pyrimidine DNA triplex.[97] Homonuclear 3D methods are very useful for RNA fragments, where considerable overlap exists for most sugar protons. Thus, most proton assignments can be obtained from a single 3D TOCSY–NOESY spectrum, as demonstrated for a 12-mer RNA duplex.[98]

Structural studies of DNA fragments can use 3D NOESY–TOCSY methods for resolving ambiguities in the assignment of cross peaks in 2D NOE spectra. Such methods have been applied for the analysis of the NOEs of a 12-mer DNA duplex containing a GG mismatch[99] and for analysis of a modified 12-mer DNA duplex.[100] In both cases the 3D spectra clarified unusual NOEs, with important consequences for the geometry.

For larger DNA and RNA fragments the HOHAHA transfer could turn out to be inefficient. In this situation 3D NOESY–NOESY is an alternative, since it is not based on a possibly weak homonuclear J-coupling, and cross relaxation becomes increasingly efficient at higher molecular weights. It has been demonstrated that 3D NOESY–NOESY spectra of good quality can be recorded for a 22-mer duplex.[11] Similarly, 3D NOESY–NOESY has been applied to a 40-base three-stranded DNA junction,[101] where it allowed the completion of the proton assignments and confirmed the unusual geometry at the junction, and to a hybrid DNA–RNA dodecamer duplex,[102] where it resolved superimposed cross peaks of the RNA strand.

24.9 PROSPECTS FOR 3D NMR SPECTROSCOPY

The NOE effect and the J-coupling can be combined in three different ways in homonuclear 3D NMR experiments. 3D experiments with a simple magnetization transfer such as in 3D COSY–COSY are most amenable for analysis. However, the linewidth of larger biomolecules is of a similar magnitude to the ^{3}J(H, H) coupling, which leads to weak 3D cross-peak intensities. Magnetization transfer by HOHAHA is less sensitive to line broadening, and is therefore preferable for most applications. Thus, spin systems of biomolecules with molecular masses below 20 kDa can be analyzed using 3D TOCSY–TOCSY and 3D NOESY–TOCSY spectra. Furthermore, these latter spectra turn out to be useful in assigning resonances and analyzing the secondary and even the tertiary structure of proteins. For biomolecules of greater mass than 20 kDa or with a large linewidth, mixing periods based on J(H, H) couplings may not be efficient. In this case 3D NOESY–NOESY or 3D ROESY–ROESY experiments can be used for resolving the overlap of cross peaks in NOESY and ROESY spectra.

The analysis of many multidimensional NMR spectra may benefit from the development of programs which allow the graphical and interactive bookkeeping of the spectra on workstations. This is particularly true for the homonuclear 3D spectra of biomolecules, where the large number of interactions and the fact that the relay is to many other nuclei often leads to many cross peaks. Since the analysis of such spectra can be complex, a practical approach where the 3D spectra assist the analysis of 2D TOCSY and NOESY spectra seems to be the most fruitful. A further improvement for all multidimensional techniques is the application of field gradient methods using shielded gradient coils. This may allow a reduction in the phase cycling for coherence selection and artifact suppression, so that spectra can be obtained with a significant higher resolution per domain. This is particularly important for the automated analysis of multidimensional spectra, where a large tolerance in the coordinates of a cross peak due to low resolution may result in a large number of possible assignments.

Another class of 3D NMR experiments, not discussed in detail in the present overview, is formed by the heteronuclear 3D NMR experiments, such as 3D TOCSY–HMQC and 3D NOESY–HMQC. These methods also use a third dimension to increase the resolution. Compared with the homonuclear proton methods they have the advantage of an efficient J transfer due to the large ^{15}N–^{1}H and ^{13}C–^{1}H coupling constants. For sufficient sensitivity, it is generally necessary to

obtain isotopically enriched biological material. For doubly (^{13}C, ^{15}N) labeled proteins and ^{13}C labeled oligonucleotides straightforward and powerful methods have been developed both for assigning resonances and for structural studies (see Clore and Gronenborn[19] and Oschkinat *et al*.[21] for reviews). In many cases, however, labeling may be impossible to realize, and then homonuclear 3D methods are still possible. In other cases only ^{15}N labeling may feasible. It is then possible to record 3D TOCSY–NOESY–(^{15}N, ^{1}H)–HSQC spectra[103,104] or 4D TOCSY–NOESY–(^{15}N, ^{1}H)–HSQC spectra[105] to resolve ambiguities in 3D NOESY–(^{15}N, ^{1}H)–HSQC spectra. It turns out that the analysis of such spectra is very similar to that of the homonuclear 3D TOCSY–NOESY spectra.

During the past few years many homonuclear and heteronuclear 3D NMR experiments have been developed. These methods can complement each other and should be explored to their limits for studying larger and more complex biomolecular systems.

RELATED ARTICLES IN THE ENCYCLOPEDIA OF MAGNETIC RESONANCE

Protein Hydration

REFERENCES

1. K. Wüthrich, *NMR of Proteins and Nucleic Acids*, Wiley, New York, 1986.
2. R. R. Ernst, G. Bodenhausen, and A. Wokaun, *Principles of Nuclear Magnetic Resonance in One and Two Dimensions*, Clarendon Press, Oxford, 1987.
3. H. D. Plant, T. H. Mareci, M. D. Cockman, and W. S. Brey, *27th Experimental NMR Conference, Baltimore, Maryland, April 13–17, 1986*.
4. G. W. Vuister and R. Boelens, *J. Magn. Reson.*, 1987, **73**, 328.
5. C. Griesinger, O. W. Sørensen, and R. R. Ernst, *J. Magn. Reson.*, 1987, **73**, 574.
6. C. Griesinger, O. W. Sørensen, and R. R. Ernst, *J. Am. Chem. Soc.*, 1987, **109**, 7227.
7. H. Oschkinat, C. Griesinger, P. J. Kraulis, O. W. Sørensen, R. R. Ernst, A. M. Gronenborn, and G. M. Clore, *Nature*, 1988, **332**, 374.
8. G. W. Vuister, R. Boelens, and R. Kaptein, *J. Magn. Reson.*, 1988, **80**, 176.
9. L. E. Kay, G. M. Clore, A. Bax, and A. M. Gronenborn, *Science*, 1990, **249**, 411.
10. G. M. Clore, L. E. Kay, A. Bax, and A. M. Gronenborn, *Biochemistry*, 1991, **30**, 12.
11. R. Boelens, G. W. Vuister, T. M. G. Koning, and R. Kaptein, *J. Am. Chem. Soc.*, 1989, **111**, 8525.
12. S. W. Fesik and E. R. P. Zuiderweg, *J. Magn. Reson.*, 1988, **78**, 588.
13. E. R. P. Zuiderweg and S. W. Fesik, *Biochemistry*, 1989, **28**, 2387.
14. D. Marion, L. E. Kay, S. W. Sparks, D. A. Torchia, and A. Bax, *J. Am. Chem. Soc.*, 1989, **111**, 1515.
15. D. Marion, P. C. Driscoll, L. E. Kay, P. T. Wingfield, A. Bax, A. M. Gronenborn, and G. M. Clore, *Biochemistry*, 1989, **28**, 6150.
16. G. T. Montelione and G. Wagner, *J. Magn. Reson.*, 1990, **87**, 183.
17. M. Ikura, L. E. Kay, and A. Bax, *Biochemistry*, 1990, **29**, 4659.
18. C. Griesinger, O. W. Sørensen, and R. R. Ernst, *J. Magn. Reson.*, 1989, **84**, 14.
19. G. M. Clore and A. M. Gronenborn, *Prog. Nucl. Magn. Reson. Spectrosc.*, 1991, **23**, 43.
20. A. Bax and S. Grzesiek, *Acc. Chem. Res.*, 1993, **26**, 131.
21. H. Oschkinat, T. Müller, and T. Dieckmann, *Angew. Chem., Int. Ed. Engl.*, 1994, **33**, 277.
22. O. W. Sørensen, *J. Magn. Reson.*, 1990, **89**, 210.
23. G. W. Eich, G. Bodenhausen, and R. R. Ernst, *J. Am. Chem. Soc.*, 1982, **104**, 3731.
24. P. H. Bolton and G. Bodenhausen, *Chem. Phys. Lett.*, 1982, **89**, 139.
25. G. Wagner, *J. Magn. Reson.*, 1984, **57**, 497.
26. F. J. M. Van der Ven, C. A. G. Haasnoot, and C. W. Hilbers, *J. Magn. Reson.*, 1985, **61**, 181.
27. H. Kessler, G. Gemmecker, and S. Steuernagel, *Angew. Chem., Int. Ed. Engl.*, 1988, **100**, 600.
28. P. De Waard, R. Boelens, G. W. Vuister, and J. F. G. Vliegenthart, *J. Am. Chem. Soc.*, 1990, **112**, 3232.
29. H. Kessler, G. Gemmecker, and B. Haase, *J. Magn. Reson.*, 1988, **77**, 401.
30. W. P. Aue, E. Bartholdi, and R. R. Ernst, *J. Chem. Phys.*, 1976, **64**, 2229.

31. J. Jeener, B. H. Meier, P. Bachmann, and R. R. Ernst, *J. Chem. Phys.*, 1979, **71**, 4546.
32. S. Macura and R. R. Ernst, *Mol. Phys.*, 1980, **41**, 95.
33. A. Kumar, G. Wagner, R. R. Ernst, and K. Wüthrich, *J. Am. Chem. Soc.*, 1981, **103**, 3654.
34. A. A. Bothner-By, R. L. Stephens, J. Lee, C. D. Warren, and R. W. Jeanloz, *J. Am. Chem. Soc.*, 1984, **106**, 811.
35. A. Bax and D. G. Davies, *J. Magn. Reson.*, 1985, **65**, 355.
36. H. Oschkinat, C. Cieslar, A. M. Gronenborn, and G. M. Clore, *J. Magn. Reson.*, 1989, **81**, 212.
37. H. Oschkinat, C. Cieslar, T. A. Holak, G. M. Clore, and A. M. Gronenborn, *J. Magn. Reson.*, 1989, **83**, 450.
38. J. Cavanagh and M. Rance, *Prog. Nucl. Magn. Reson. Spectrosc.*, 1993, **27**, 1.
39. F. Ni, *J. Magn. Reson.*, 1992, **100**, 391.
40. C. Griesinger, G. Otting, K. Wüthrich, and R. R. Ernst, *J. Am. Chem. Soc.*, 1988, **110**, 7870.
41. R. Boelens, C. Griesinger, L. E. Kay, D. Marion, and E. R. P. Zuiderweg, *Nato ASI Ser., Ser. A*, 1991, **A225**, 127.
42. J.-P. Simorre and D. Marion, *J. Magn. Reson.*, 1991, **94**, 426.
43. H. Barkhuizen, R. deBeer, W. M. M. J. Bovee, and D. van Ormondt, *J. Magn. Reson.*, 1985, **61**, 465.
44. H. Gesmar, J. J. Led, and F. Abildgaard, *Prog. Nucl. Magn. Reson. Spectrosc.*, 1990, **22**, 255.
45. G. Zhu and A. Bax, *J. Magn. Reson.*, 1990, **90**, 405.
46. M. Robin, M.-A. Delsuc, E. Guitet, and J.-Y. Lallemand, *J. Magn. Reson.*, 1991, **92**, 645.
47. E. T. Olejniczak and H. L. Eaton, *J. Magn. Reson.*, 1990, **87**, 628.
48. D. Marion and A. Bax, *J. Magn. Reson.*, 1989, **83**, 205.
49. R. Saffrich, W. Beneicke, K.-P. Neidig, and H. R. Kalbitzer, *J. Magn. Reson. B*, 1993, **101**, 304.
50. L. Mitschang, C. Cieslar, T. A. Holak, and H. Oschkinat, *J. Magn. Reson.*, 1991, **92**, 208.
51. G. Otting, H. Widmer, G. Wagner, and K. Wüthrich, *J. Magn. Reson.*, 1986, **66**, 187.
52. D. Marion and A. Bax, *J. Magn. Reson.*, 1988, **79**, 352.
53. P. J. Kraulis, *J. Magn. Reson.*, 1989, **84**, 627.
54. G. J. Kleywegt, G. W. Vuister, A. Padilla, R. M. A. Knegtel, R. Boelens, and R. Kaptein, *J. Magn. Reson.*, 1993, **102**, 166.
55. M. Kjaer, K. V. Andersen, S. Ludvigsen, H. Shen, P. Windekinde, B. Sørensen, and F. M. Poulson, *Nato ASI Ser., Ser. A*, 1991, **A225**, 291.
56. K.-P. Neidig, R. Saffrich, M. Lorenz, and H. R. Kalbitzer, *J. Magn. Reson.*, 1990, **89**, 543.
57. C. Cieslar, T. A. Holak, and H. Oschkinat, *J. Magn. Reson.*, 1990, **87**, 400.
58. H. Oschkinat, T. A. Holak, and C. Cieslar, *Biopolymers*, 1991, **31**, 699.
59. R. E. Hoffman and D. B. Davies, *J. Magn. Reson.*, 1988, **80**, 337.
60. P. A. Mirau, S. A. Heffner, and F. A. Bovey, *J. Magn. Reson.*, 1990, **89**, 572.
61. C. Griesinger, O. W. Sørensen, and R. R. Ernst, *J. Chem. Phys.*, 1986, **85**, 6387.
62. Y. Yang, A. Hagemeyer, K. Zemke, and H. W. Spiess, *J. Chem. Phys.*, 1990, **93**, 7740.
63. B. S. Arun Kumar and S. J. Opella, *J. Magn. Reson.*, 1993, **101**, 333.
64. G. W. Vuister, Ph.D. Thesis, Utrecht University, 1990.
65. S. S. Wijmenga and C. P. M. van Mierlo, *Eur. J. Biochem.*, 1991, **195**, 807.
66. G. W. Vuister, R. Boelens, A. Padilla, G. J. Kleywegt, and R. Kaptein, *Biochemistry*, 1990, **29**, 1829.
67. H. Oschkinat, C. Cieslar, and C. Griesinger, *J. Magn. Reson.*, 1990, **86**, 453.
68. A. Padilla, G. W. Vuister, R. Boelens, G. J. Kleywegt, A. Cavé, J. Parello, and R. Kaptein, *J. Am. Chem. Soc.*, 1990, **112**, 5024.
69. X. Gao and W. Burkhart, *Biochemistry*, 1991, **30**, 7730.
70. J.-P. Simorre, A. Caille, D. Marion, D. Marion, and M. Ptak, *Biochemistry*, 1991, **30**, 11 600.
71. M. van de Kamp, G. W. Canters, S. S. Wijmenga, A. Lommen, C. W. Hilbers, H. Nar, A. Messerschmidt, and R. Huber, *Biochemistry*, 1992, **31**, 10 194.
72. D. Morikis, C. A. Lepre, and P. E. Wright, *Eur. J. Biochem.*, 1994, **219**, 611.
73. J. N. Breg, L. Sarda, P. J. Cozzone, R. Boelens, and R. Kaptein, *Eur. J. Biochem.*, 1995, **227**, 663.

74. R. Fogh, G. Ottleben, H. Rüterjans, M. Schnarr, R. Boelens, and R. Kaptein, *EMBO J.*, 1994, **13**, 3936.
75. X. Qian, S. N. Gozani, H. S. Yoon, C. J. Jeon, K. Agarwal, and M. A. Weiss, *Biochemistry*, 1993, **32**, 9944.
76. C. Cieslar, T. A. Holak, and H. Oschkinat, *J. Magn. Reson.*, 1990, **87**, 184.
77. J. N. Breg, R. Boelens, G. W. Vuister, and R. Kaptein, *J. Magn. Reson.*, 1990, **87**, 646.
78. A. Padilla, *Cahiers IMABIO CNRS (Paris)*, 1992, **3**, 19.
79. A. Ross, J. Freund, C. Cieslar, H. Oschkinat, M. Schleicher, and T. A. Holak, *J. Magn. Reson.*, 1991, **95**, 567.
80. G. W. Vuister, R. Boelens, A. Padilla, and R. Kaptein, *J. Biomol. NMR*, 1991, **1**, 421.
81. D. Marion and F. Guerlesquin, *Biochemistry*, 1992, **31**, 8171.
82. T. A. Holak, J. Habazettl, H. Oschkinat, and J. Otlewski, *J. Am. Chem. Soc.*, 1991, **113**, 3196.
83. P. de Waard, B. R. Leeflang, J. F. G. Vliegenthart, R. Boelens, G. W. Vuister, and R. Kaptein, *J. Biomol. NMR*, 1992, **2**, 211.
84. H. Kessler, S. Seip, and J. Saulitis, *J. Biomol. NMR*, 1991, **1**, 83.
85. J. Habazettl, A. Ross, H. Oschkinat, and T. A. Holak, *J. Magn. Reson.*, 1992, **97**, 511.
86. A. M. J. J. Bonvin, R. Boelens, and R. Kaptein, *J. Magn. Reson.*, 1991, **95**, 626.
87. A. M. J. J. Bonvin, R. Boelens, and R. Kaptein, in *Computer Simulation of Biomolecular Systems*, eds. W. F. van Gunsteren, P. K. Weiner, and A. J. Wilkinson, Escom, Leiden, 1993, Vol. 2, p. 403.
88. P. Yip and D. A. Case, *J. Magn. Reson.*, 1989, **83**, 643.
89. A. M. J. J. Bonvin, R. Boelens, and R. Kaptein, *J. Biol. NMR*, 1991, **1**, 305.
90. J. Habazettl, M. Schleicher, J. Otlewski, and T. A. Holak, *J. Mol. Biol.*, 1992, **228**, 156.
91. R. Bernstein, A. Ross, C. Cieslar, and T. A. Holak, *J. Magn. Reson.*, 1993, **101**, 185.
92. G. Otting and K. Wüthrich, *J. Am. Chem. Soc.*, 1989, **111**, 1871.
93. G. Otting, E. Liepinsh, B. T. Farmer II, and K. Wüthrich, *J. Biomol. NMR*, 1991, **1**, 209.
94. T. A. Holak, R. Witscheck, and A. Ross, *J. Magn. Reson.*, 1992, **97**, 632.
95. G. W. Vuister, P. de Waard, R. Boelens, J. F. G. Vliegenthart, and R. Kaptein, *J. Am. Chem. Soc.*, 1989, **111**, 772.
96. M. M. W. Mooren, C. W. Hilbers, G. A. van der Marel, J. H. van Boom, and S. S. Wijmenga, *J. Magn. Reson.*, 1991, **94**, 101.
97. I. Radhakrishnan, D. J. Patel, and X. Gao, *Biochemistry*, 1992, **31**, 2514.
98. S. S. Wijmenga, H. A. Heus, B. Werten, G. A. van der Marel, J. H. van Boom, and C. W. Hilbers, *J. Magn. Reson.*, 1994, **103**, 134.
99. M. E. Piotto and D. G. Gorenstein, *J. Am. Chem. Soc.*, 1991, **113**, 1438.
100. X. Gao and P. W. Jeffs, *J. Biomol. NMR*, 1994, **4**, 17.
101. M. A. Rosen and D. J. Patel, *Biochemistry*, 1993, **32**, 6563.
102. X. Gao and P. W. Jeffs, *J. Biomol. NMR*, 1994, **4**, 367.
103. L. Mueller, S. Campbell-Burk, and P. Domaille, *J. Magn. Reson.*, 1992, **96**, 408.
104. S. Boentges, J. M. Schmidt, T. Levante, and R. R. Ernst, *15th International Conference on Magnetic Resonance in Biological Systems, Jerusalem, Israel, August 1992*.
105. R. Boelens, *Cahiers IMABIO CNRS (Paris)*, 1992, **3**, 33.